Submitted to the
XXII International Symposium on Lepton-Photon Interactions at High Energy
30 June - 5 July, Uppsala, Sweden

Abstract: 291 **Session: QCD/HS**

Diffractive photoproduction of J/ψ mesons with large momentum transfer at HERA

ZEUS Collaboration

Abstract

The proton-dissociative diffractive photoproduction of J/ψ mesons has been studied in ep collisions with the ZEUS detector at HERA using an integrated luminosity of 112 pb^{-1}. The cross section has been measured as a function of the centre-of-mass energy of the photon-proton system and of the squared four-momentum transfer at the proton vertex. The results are compared to perturbative QCD calculations based on the BFKL and DGLAP evolution equations.

1 Introduction

General properties of proton-dissociative photoproduction of vector mesons at large squared four-momentum transfer, t, have been successfully described by pQCD-based models where a quasi-real photon fluctuates into a $q\bar{q}$ pair which then interacts with a single parton in the proton via colour singlet exchange. Such an exchange can be either two gluons [1] (Fig. 1a) or a gluon ladder (Fig. 1b). The latter can be described by standard DGLAP [2] or BFKL [3–5] QCD evolution equations.

In pQCD models, t, or the vector meson mass in the case of the J/ψ, provide a large energy scale required for the perturbative treatment of QCD processes. In particular, the pQCD models predict t distributions that are relatively hard compared to those observed in elastic vector meson photoproduction. A model using BFKL exchange describes well the shapes and magnitude of the differential cross section as a function of t for ρ, ϕ and J/ψ mesons [6].

The pQCD models differ in the predicted energy dependence of $d\sigma/dt$: two-gluon exchange yields energy independent cross sections [1], gluon ladder exchange based on DGLAP evolution predicts practically no energy dependence [2] while BFKL evolution leads to cross sections that rise significantly with increasing energy [4,5]. A rise has been observed in J/ψ photoproduction at $|t| > 5\,\mathrm{GeV}^2$ [7] suggesting the onset of BFKL dynamics at larger $|t|$. This rise is investigated in this paper in which the differential cross section $d\sigma/dt$ and its energy dependence is presented for the diffractive photoproduction process, $\gamma p \rightarrow J/\psi\ Y$, where Y is the proton dissociative system. The data cover the photon-proton centre-of-mass (CMS) energy range of $50 < W < 150\,\mathrm{GeV}$, $M_Y < 30\,\mathrm{GeV}$ and extend up to $|t| = 20\,\mathrm{GeV}^2$. The results are compared to predictions from the BFKL model [5] and DGLAP calculations in the leading logarithmic approximation [2].

2 Experimental conditions

The data used in this analysis were collected in 1996 - 2000 from ep interactions with the ZEUS detector [8] at HERA, which operated with a proton beam energy of 820(920) GeV and a positron/electron beam energy of 27.5 GeV, and correspond to an integrated luminosity of $112\,\mathrm{pb}^{-1}$. The main components used for this analysis are the central tracking detector (CTD) [9], the uranium-scintillator calorimeter (CAL) [10], the muon chambers [11], the proton remnant tagger (PRT) [12] and the forward plug calorimeter (FPC) [13].

3 Kinematics and cross sections

The process in question is proton-dissociative J/ψ production in ep interactions,

$$e(k)p(P) \to e(k')J/\psi(v)Y(P')$$

where k, k', P, P' and v are the four-momenta of the incident positron, scattered positron, incident proton, diffractive nucleonic system Y, and J/ψ, respectively (Fig. 2). The kinematic variables used to describe this process are:

- $Q^2 = -q^2 = -(k-k')^2$, the negative squared four-momentum of the exchanged photon;
- $W^2 = (q + P)^2$, the squared centre-of-mass energy of the photon-proton system;
- $-t = (P' - P)^2 = (v - q)^2$, the squared four-momentum transfer at the proton vertex;
- $z = (P \cdot v)/(P \cdot q)$, the event elasticity, i.e. the fraction of virtual photon energy transferred to the J/ψ in the proton rest frame.

The kinematic variables were reconstructed using the momenta of the J/ψ decay products.

For the photon virtualities, $Q^2 \approx 0.07\,\mathrm{GeV}^2$, covered by this measurement, the differential ep cross section can be expressed as

$$\frac{d^2\sigma^{ep\to eJ/\psi Y}}{dydQ^2} = \Gamma_T(y, Q^2)\sigma^{\gamma p}(y)$$

where y is the fraction of the electron energy transferred to the hadronic final state (in the proton rest frame) and Γ_T is the flux of the transverse virtual photons. The photon-proton cross section can be extracted from the ep cross section. The ep and γp cross sections are related to each other by means of the flux factor generated at the leptonic vertex. The flux factor can be integrated over the y and Q^2 covered by the measurement.

4 Reconstruction and selection of events

The signature of proton dissociative J/ψ photoproduction, $ep \to eJ/\psi\ Y$, consists of two oppositely charged muons from J/ψ decay, the dissociated proton and the lack of the scattered electron in the main detector. The electron is scattered through a small angle and escapes undetected down the beampipe. The low mass hadronic states originating from the scattered proton are registered in the forward[1] part of the calorimeter or in other forward detectors.

[1] The ZEUS coordinate system is right-handed Cartesian system, with the Z axis pointing in the proton beam direction, referred to as a the 'forward direction', and the X axis pointing left towards the centre of HERA. The coordinate origin is at the nominal interaction point.

The events were selected online by the ZEUS trigger system. The di-muon sample was triggered by requiring at least one track in the CTD matched to an energy deposit in the CAL. The energy deposit was required to be consistent with a minimum ionising particle and associated to a signal in the muon chambers.

Further selection made offline required two energy deposits in the CAL associated with the two candidate muons from the J/ψ decay. To select events in which the proton dissociates, an energy deposit above 400 MeV with $|\eta| > 2.1$ in the forward part of the CAL was required in conjunction with either a signal in the PRT (for 1996-1997 data sample) or an energy deposit above 1 GeV in the FPC (for 1998-2000 data sample). Events with additional energy deposits with $|\eta| < 2.1$ above the noise level (300 MeV) and not associated with lepton candidates were rejected.

In order to compare the cross sections with theoretical predictions and previous measurements, an additional cut of $z > 0.95$ was applied. This ensures the diffractive nature of the interaction and also restricts the invariant mass of the system Y to be $M_Y < 30\,\mathrm{GeV}$ through the relation $z = 1 - (M_Y^2 - t)/W^2$. The measurement of z is obtained from $(E - p_z)_{J/\psi}/\Sigma(E - p_z)$ where $\Sigma(E - p_z)$ is calculated from all energy deposits in the CAL above the noise level including the decay products of the J/ψ.

Since the typical Q^2 is small, it can be neglected in the reconstruction of the other kinematic variables. In particular, $|t|$ was assumed to be equal to the squared transverse-momentum of the di-muon system resulting from the J/ψ decay. Events were required to be in a kinematic range where the properties of the final state particles are well measured and the acceptance is well defined, which is satisfied for $1 < |t| < 20\,\mathrm{GeV}^2$ and $40 < W < 160\,\mathrm{GeV}$.

5 Monte Carlo simulation

The acceptance and the effects of the detector response were determined using samples of Monte Carlo (MC) events. All generated events were passed through the standard ZEUS detector simulation, based on GEANT 3.13 [14] program, the ZEUS trigger simulation package, and through the same reconstruction and analysis programs as the data.

The process $ep \to e\ J/\psi\ Y$ was modelled using the generator EPSOFT [15, 16]. The $\gamma p \to J/\psi\ Y$ cross section was parametrised as $f(t)(M_Y^2)^{-\beta(t)}$. The MC samples were tuned to describe the FCAL and FPC energy distributions, which are sensitive to M_Y, yielding $\beta(t) = \exp(0.25 - 0.37|t|)$. The MC t distribution was also reweighted to obtain the power-like dependence of $d\sigma/dt$ as measured in the data.

A non-resonant background arising from the $\gamma\gamma$ fusion process, $ep \to e\ \mu^+\mu^-\ Y$, where one of the photons is emitted by the electron and the second photon is radiated off the proton was simulated using the generator GRAPE-DILEPTON 1.1 [17].

6 Results

The invariant mass distribution of the $\mu^+\mu^-$ pairs is presented in Fig. 3. The MC distribution of the J/ψ signal is also shown as well as the non-resonant background. After all selection cuts almost 3000 di-muon events were left in the mass range $2.6 < M_{\mu^+\mu^-} < 3.5$ GeV. The non-resonant background was estimated in each bin using GRAPE, normalised to the luminosity of the data.

The systematic uncertainties on the measured cross sections were determined by varying the selection cuts and by modifying the analysis procedure. The main source of the systematic uncertainties (about 10%) comes from the corrections for the muon trigger efficiency. The systematic uncertainties are smaller than the statistical errors.

The differential cross section $d\sigma(\gamma p \to J/\psi\ Y)/d|t|$ was measured as a function of $|t|$ in the range $50 < W < 150\,\text{GeV}$. The data are compared to the H1 measurement [7], as shown in Fig. 4. The cross section, for $|t| < 6\,\text{GeV}^2$, tends to lie above the H1 data. In Fig. 5 the $|t|$ dependence is compared with theoretical predictions from the different pQCD models. The model based on BFKL evolution [5] provides calculations in the leading logarithmic (LL) approximation as well as with non-leading corrections (nonL). The latter has been used to make predictions for both fixed and running α_s. The model based on DGLAP evolution gives predictions in the LL approximation [2] in the range of the model validity ($|t| < M^2_{J/\psi}$). The parameters of both pQCD models are those which best describe previous HERA measurements [7]. The BFKL LL and BFKL nonL predictions with fixed α_s as well as the DGLAP LL calculations generally describe the $|t|$ dependence of the cross section but rather underestimate its magnitude, while the BFKL nonL calculations with running α_s give a steeper $|t|$ dependence and are unable to describe the data across the whole range of $|t|$.

The cross section $\sigma^{\gamma p \to J/\psi\ Y}$ was measured as a function of W in four bins of $|t|$ as shown in Fig. 6. The cross sections were fitted to a dependence $\sigma \propto W^{\delta}$. The extracted values of δ increase with rising $|t|$ and show similar behaviour to that reported previously [7]. In the Regge formalism, the differential cross section can be expressed as $d\sigma/dt \propto W^{4(\alpha_{IP}(t)-1)}$, where $\alpha_{IP}(t)$ is the Pomeron trajectory. The value of $\alpha_{IP}(t)$ for each value of t can therefore be obtained from $\alpha_{IP} = (\delta + 4)/4$. The Pomeron trajectory is usually parametrised as a linear form $\alpha_{IP}(t) = \alpha_{IP}(0) + \alpha'_{IP} \cdot t$. A fit performed to the four bins of t yields an intercept $\alpha_{IP}(0) = 1.153 \pm 0.048(\text{stat.}) \pm 0.039(\text{syst.})$ and a slope $\alpha'_{IP} = -0.020 \pm 0.014(\text{stat.}) \pm 0.010(\text{syst.})$, consistent with values determined by H1 [7].

They are quite different from parametrisation of the 'soft' Pomeron [18] but are consistent with the prediction of the BFKL Pomeron [19, 20]. In Fig. 7 the comparison with the previous measurement is presented. In the range of $2 < |t| < 5\,\mathrm{GeV}^2$ the ZEUS cross sections tend to be higher than the H1 measurements and a steeper W dependence is observed. The data are also compared to the theoretical predictions in Fig. 8. Currently, the predictions are only available for $|t| > 2\,\mathrm{GeV}^2$ and, in the case of BFKL-based model, only for fixed α_s. The DGLAP LL predictions are not able to describe the W dependence while the BFKL LL predictions quantitatively reproduce the rise of the cross section.

To summarise, the differential cross section $d\sigma/dt$ for proton-dissociative J/ψ photoproduction is reproduced by the BFKL LL and nonL calculations with fixed α_s. The predictions of the same model, but with running α_s, are too steep. The data for $|t| < M^2_{J/\psi}$ are well described by the model based on DGLAP evolution. The cross section rises significantly with a rise markedly faster for $|t| > 2\,\mathrm{GeV}^2$. This behaviour is reproduced by the BFKL-based model but not by the DGLAP calculations. An effective Pomeron trajectory was estimated, yielding an intercept $\simeq 1.15$ and a slope consistent with zero.

References

[1] D. Yu. Ivanov et al., Phys. Lett. **B 478**, 101 (2000).

[2] E. Gotsman et al., Phys. Lett. **B 532**, 37 (2002).

[3] J. Bartels et al., Phys. Lett. **B 375**, 301 (1996).

[4] J. R. Forshaw and G. Poludniowski, Eur. Phys. J. **C 26**, 411 (2003).

[5] R. Enberg et al., Eur. Phys. J. **C 26**, 219 (2002).

[6] ZEUS Coll., S. Chekanov et al., Eur. Phys. J. **C 26**, 389 (2003).

[7] H1 Coll., A. Aktas et al., Phys. Lett **B 568**, 205 (2003).

[8] ZEUS Coll., U. Holm (ed.), *The ZEUS Detector*. Status Report (unpublished), DESY (1993), available on `http://www-zeus.desy.de/bluebook/bluebook.html`.

[9] N. Harnew et al., Nucl. Inst. Meth. **A 279**, 290 (1989);
B. Foster et al., Nucl. Phys. Proc. Suppl. **B 32**, 181 (1993);
B. Foster et al., Nucl. Inst. Meth. **A 338**, 254 (1994).

[10] M. Derrick et al., Nucl. Inst. Meth. **A 309**, 77 (1991);
A. Andresen et al., Nucl. Inst. Meth. **A 309**, 101 (1991);
A. Caldwell et al., Nucl. Inst. Meth. **A 321**, 356 (1992);
A. Bernstein et al., Nucl. Inst. Meth. **A 336**, 23 (1993).

[11] G. Abbiendi et al., Nucl. Inst. Meth. **A 333**, 342 (1993).

[12] ZEUS Coll., J. Breitweg et al., Z. Phys. **C 75**, 421 (1997).

[13] ZEUS coll., FPC group, A. Bamberger et al., Nucl. Inst. Meth. **A 450**, 235 (2000).

[14] R. Brun et al., *GEANT 3.13*, 1987. CERN DD/EE/84-1.

[15] M. Kasprzak. Ph.D. Thesis, Warsaw Univ., Warsaw, Poland, Report DESY F35D-96-16, 1996.

[16] L. Adamczyk. Ph.D. Thesis, Univ. of Mining and Metallurgy, Cracow, Poland, Report DESY-THESIS-1999-045, 1999.

[17] T. Abe, Comp. Phys. Comm. **136**, 126 (2001).

[18] A. Donnachie and P.V. Landshoff, Phys. Lett. **B 348**, 213 (1995).

[19] S.J. Brodsky et al., JETP Lett. **70**, 155 (1999).

[20] N.N. Nikolaev, B.G. Zakharov and V.R. Zoller, Phys. Lett. **B 366**, 337 (1996).

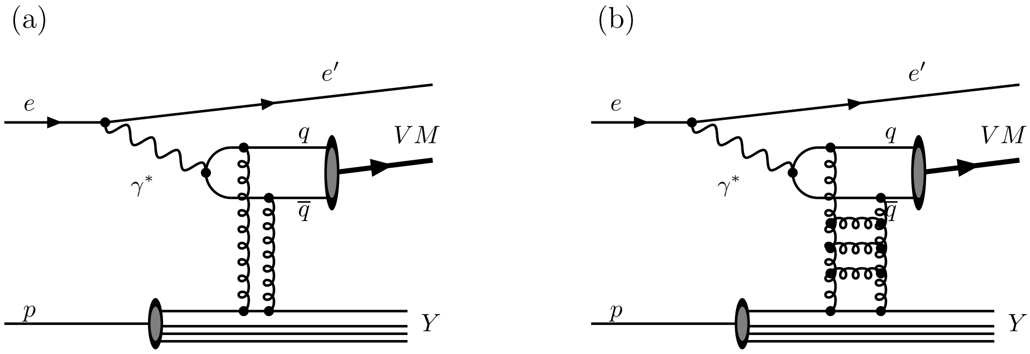

Figure 1: *(a) The pQCD diagram for proton-dissociative vector-meson electroproduction via two-gluon exchange. (b) The pQCD diagram with gluon ladder exchange.*

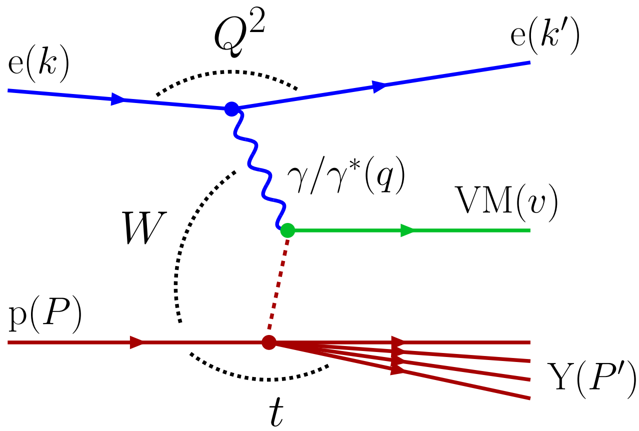

Figure 2: *Schematic diagram of proton-dissociative J/ψ production in ep interactions, $ep \to eJ/\psi\, Y$.*

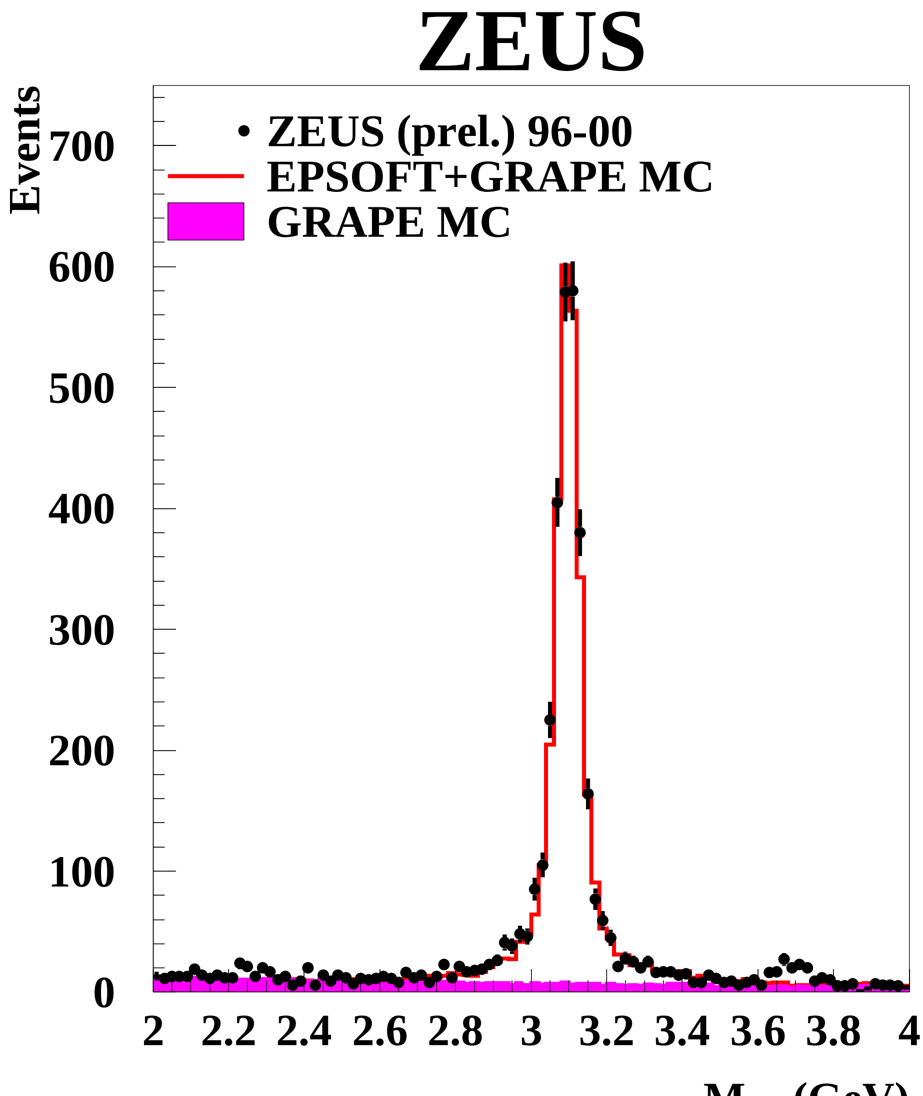

Figure 3: *The invariant mass spectrum for $J/\psi \to \mu^+\mu^-$ in the kinematic range $1 < |t| < 20\,GeV^2$, $50 < W < 150\,GeV$ and $z > 0.95$. The data are compared to the MC distributions. The shaded histogram represents the $ep \to e\mu^+\mu^- Y$ background as simulated by* GRAPE. *The open histogram represents the sum of J/ψ and background MC events.*

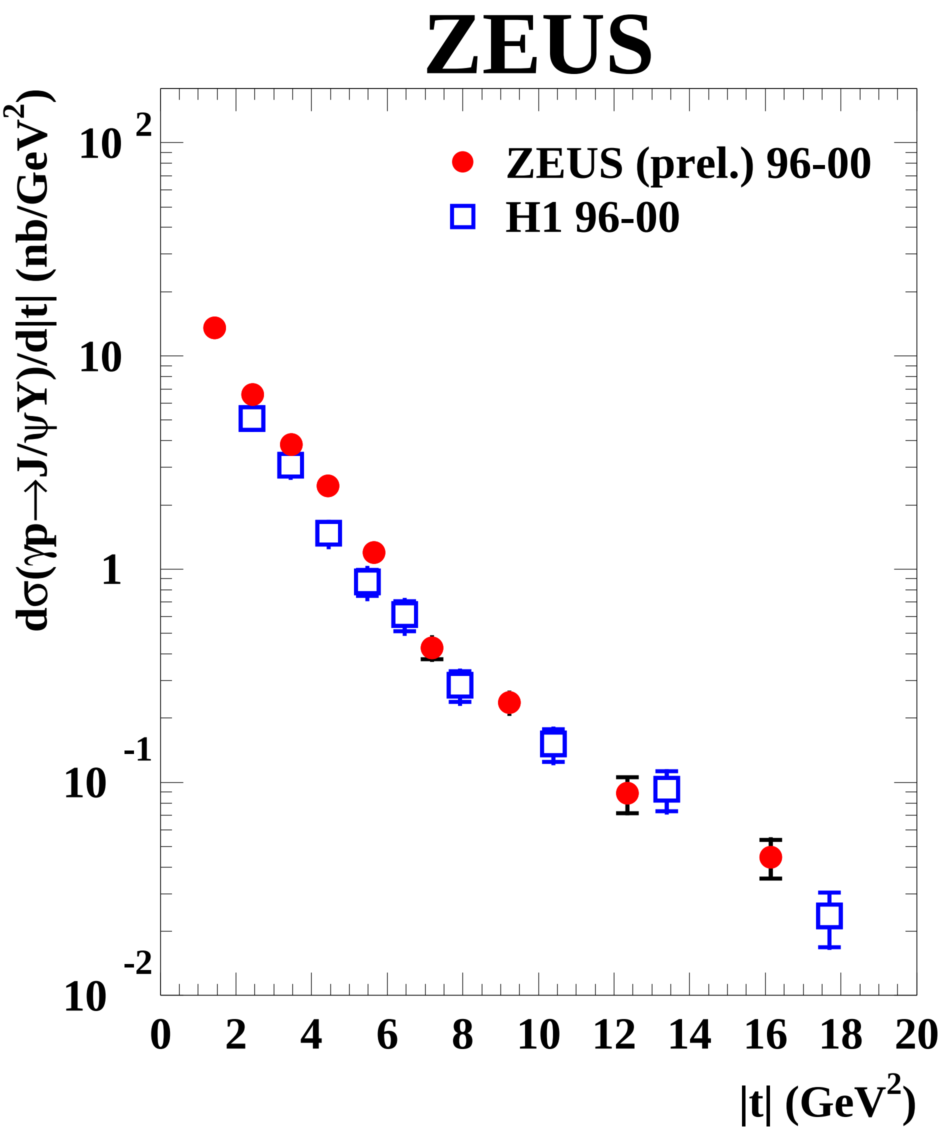

Figure 4: *The differential cross section $d\sigma/d|t|$ for the process $\gamma p \to J/\psi\ Y$ calculated for $1 < |t| < 20\ GeV^2$, $50 < W < 150\ GeV$ and $z > 0.95$. The comparison with the H1 results (open dots) is shown. The inner bars represent the statistical uncertainty and the outer represent the statistical and systematic uncertainty added in quadrature.*

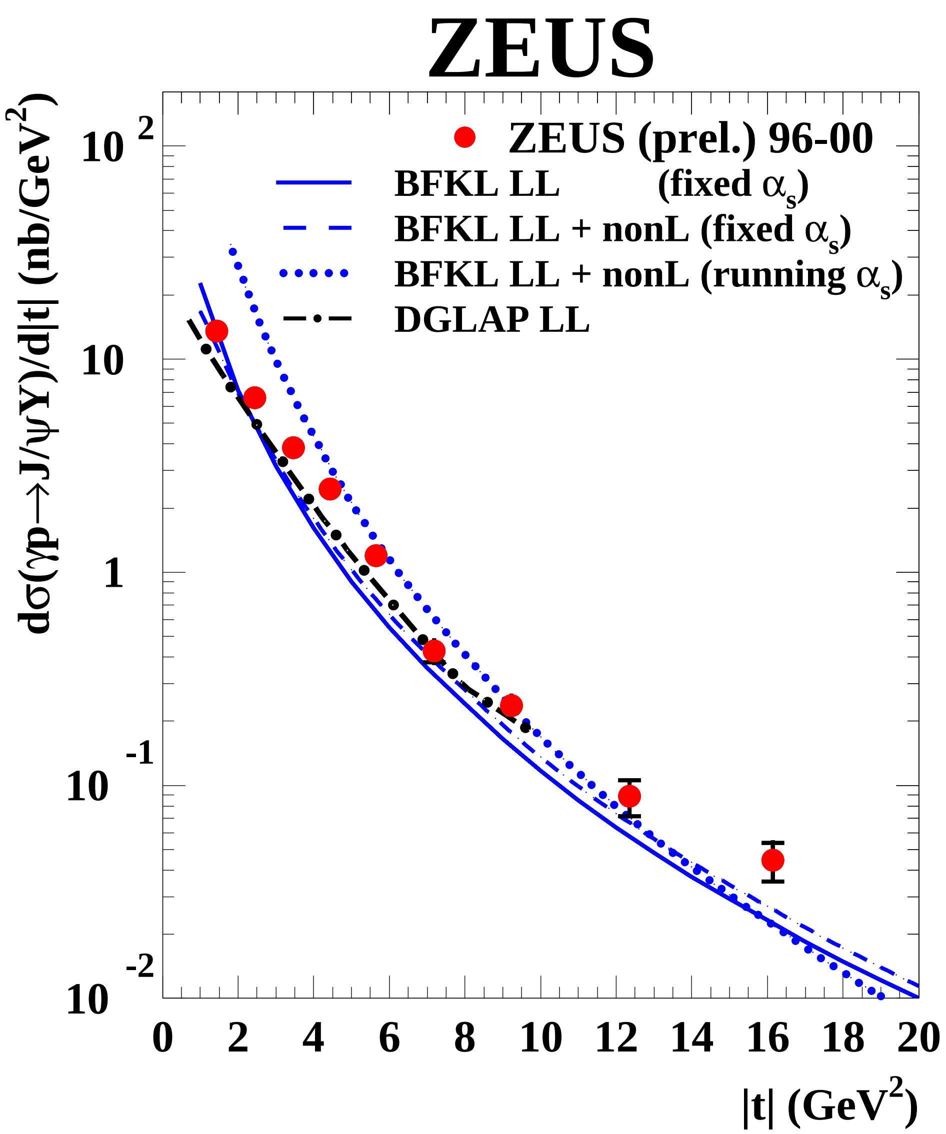

Figure 5: *The differential cross section $d\sigma/d|t|$ for the process $\gamma p \to J/\psi\ Y$ calculated for $1 < |t| < 20\,GeV^2$, $50 < W < 150\,GeV$ and $z > 0.95$. The inner bars correspond to the statistical uncertainty and the outer to the statistical and systematic uncertainty added in quadrature. The solid line represents the results of BFKL LL with fixed α_s and the dashed (dotted) line – including non-leading corrections (nonL) with fixed (running) α_s. The dashed-dotted curve is a prediction based on DGLAP LL calculations.*

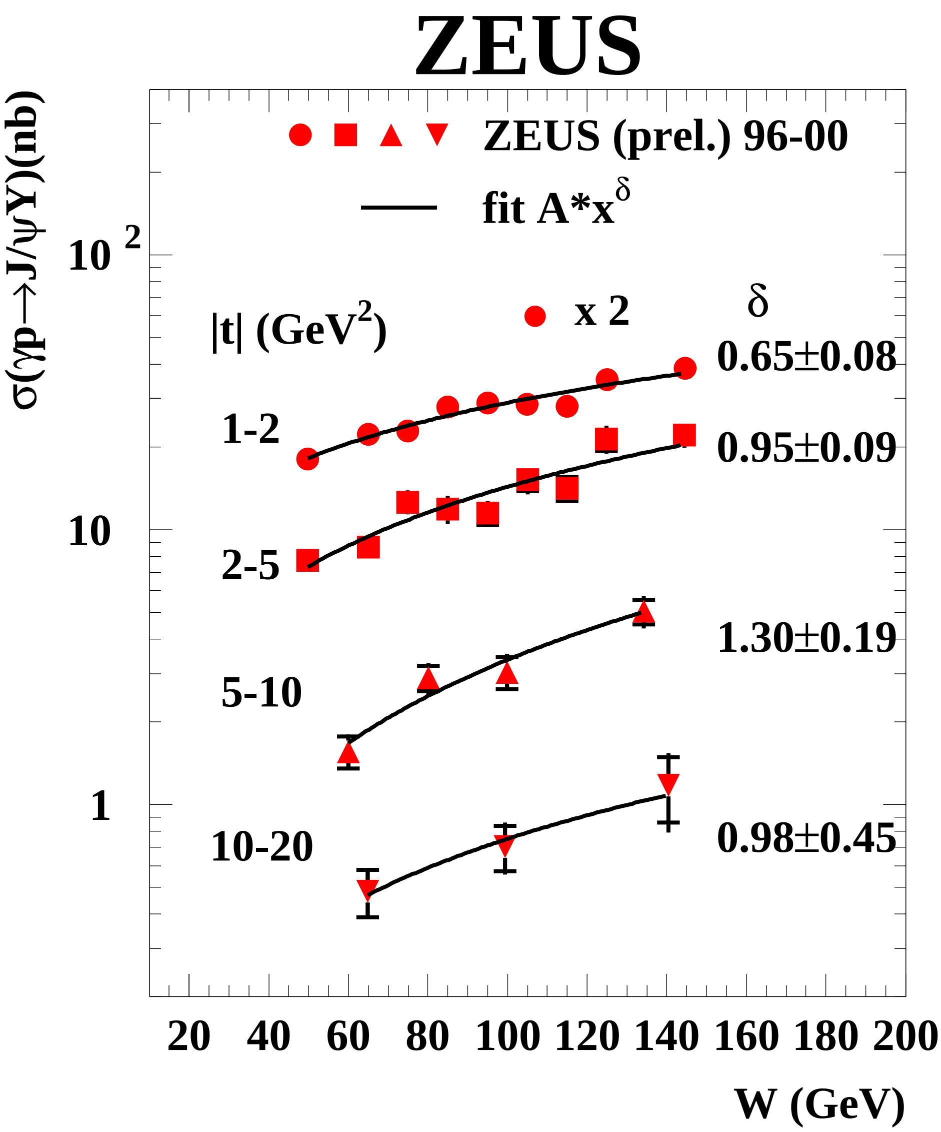

Figure 6: *The cross section as a function of W in four intervals of $|t|$ for $z > 0.95$. The inner bars correspond to the statistical uncertainty and the outer to the statistical and systematic uncertainty added in quadrature. The solid lines are the results of the fit to the form $\sigma \propto W^{\delta}$. The values of power δ are also indicated.*

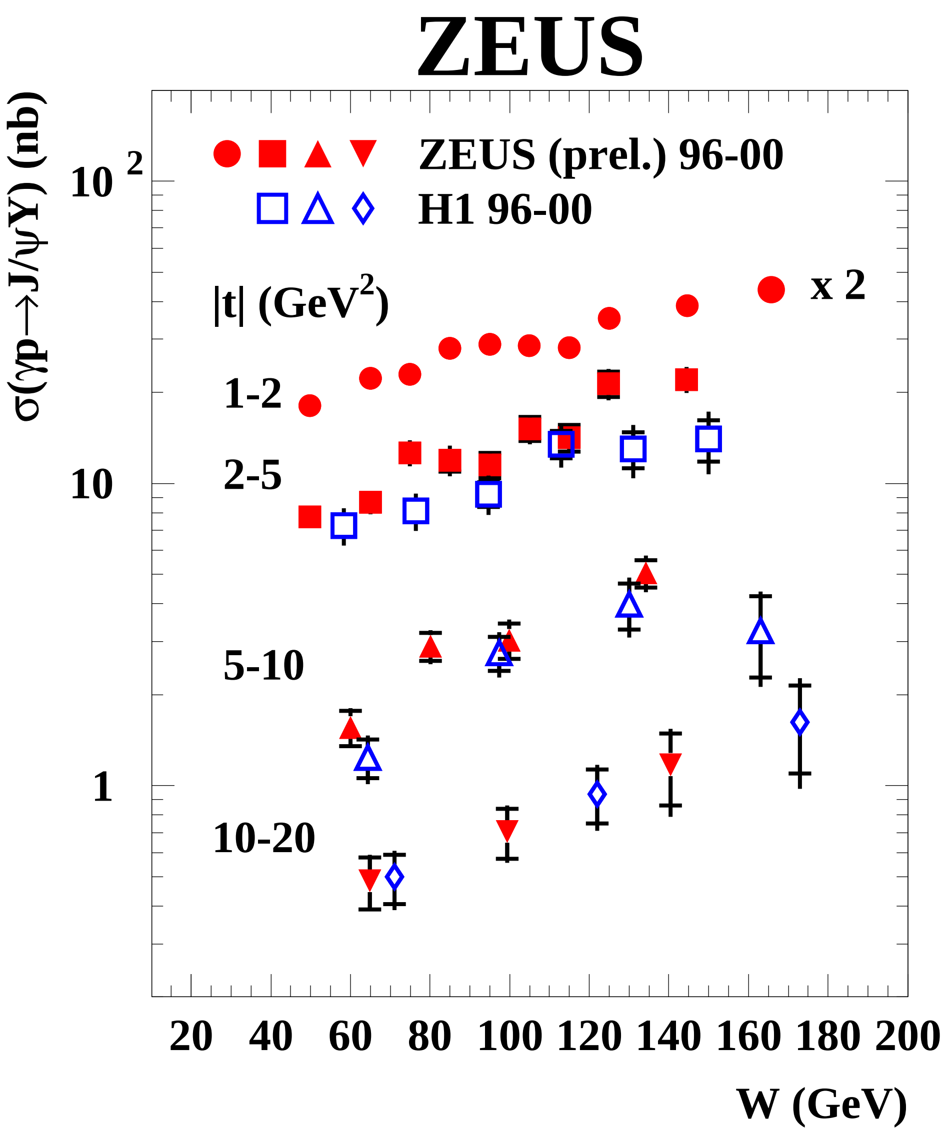

Figure 7: *The cross section as a function of W in four intervals of $|t|$ for $z > 0.95$. The inner bars correspond to the statistical uncertainty and the outer to the statistical and systematic uncertainty added in quadrature. The comparison with the H1 results is shown.*

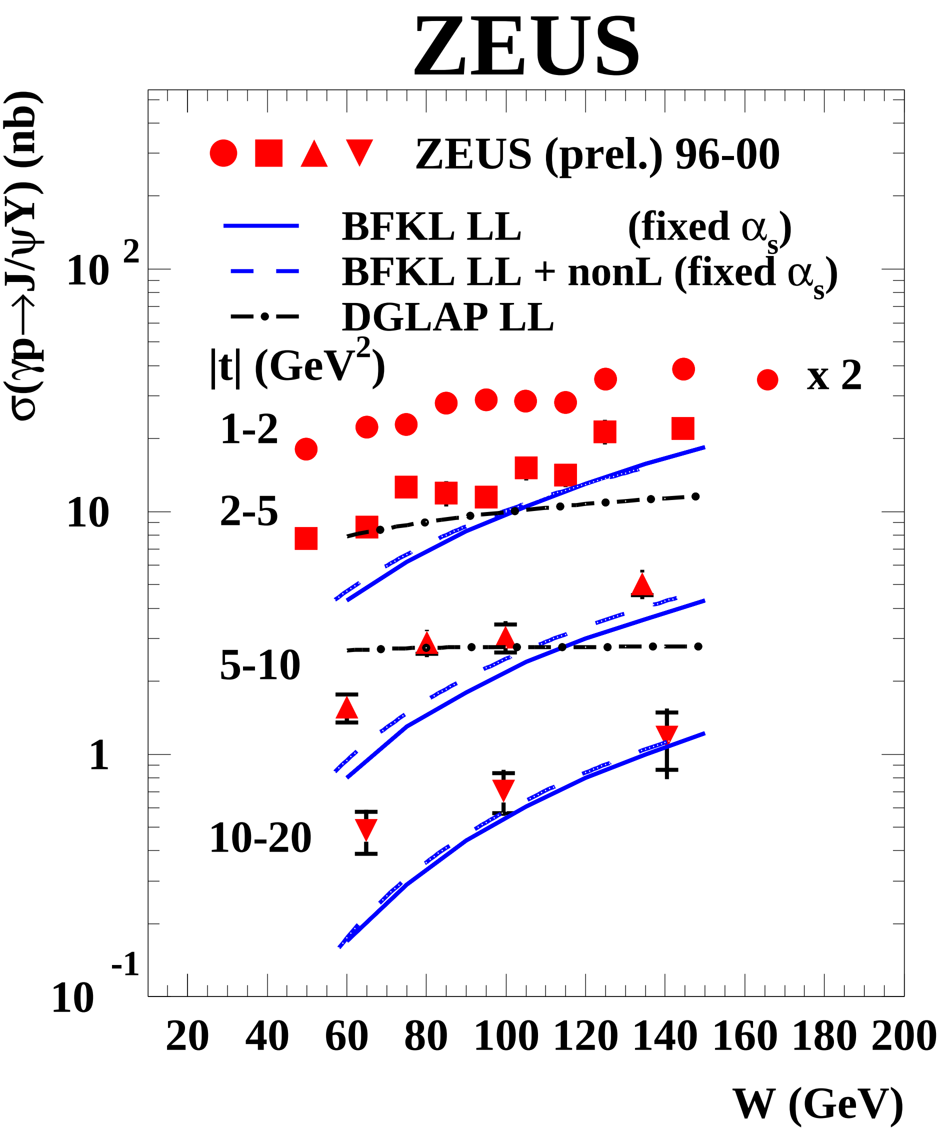

Figure 8: *The cross section as a function of W in four intervals of $|t|$ for $z > 0.95$. The inner bars correspond to the statistical uncertainty and the outer to the statistical and systematic uncertainty added in quadrature. The solid line shows the prediction of BFKL LL calculations and the dashed line corresponds to the predictions including also the nonleading corrections for fixed α_s. The dashed-dotted curve represents the DGLAP LL based calculations.*